*Desalination and Water Treatment*
www.deswater.com

doi: 10.5004/dwt.2018.21844

109 (2018) 271–278
March

# Removal of Cr(III) and Cu(II) from aqueous solution by fulvic acid functionalized magnetite nanoparticles

Chengwei Zhao[a], Hongguang Guo[a,b,*], Yongli Zhang[a], Weihong Tang[a], Yang Liu[a], Xin Cheng[a], Wei Li[a]

[a]*College of Architecture and Environment, Sichuan University, Chengdu 610065, China, Tel. +86-028-85408889; Fax: +86-028-85405534; emails: hgguo@scu.edu.cn (H. Guo), 1097802729@qq.com (C. Zhao), xyl_scu@126.com (Y. Zhang), 476273789@qq.com (W. Tang), 237668713@qq.com (Y. Liu), 527656183@qq.com (X. Cheng), 1229301513@qq.com (W. Li)*
[b]*Department of Civil and Environmental Engineering, University of Washington, Box 352700, Seattle, WA 98195-2700, United States*

Received 8 June 2017; Accepted 22 December 2017

**ABSTRACT**

Novel $Fe_3O_4$ nanoparticles coated with fulvic acid (FA-$Fe_3O_4$) were developed to remove selected metals ($Cr^{3+}$ and $Cu^{2+}$) from water. Taking advantage of the chelation between the functional groups of FA and iron, FA-$Fe_3O_4$ nanoparticles were synthesized via the chemical coprecipitation method. The multiple characterizations indicated that FA was successfully bonded onto $Fe_3O_4$ through carboxyl and carbonyl, with a stable performance. It was demonstrated that nanoscale material with an average size of 15 nm and a specific surface area of 55.16 $m^2/g$ was obtained through scanning electron microscopy and Brunauer–Emmett–Teller characterization. The adsorption experiments indicated that the adsorption capability for $Cr^{3+}$ and $Cu^{2+}$ were 11.59 and 3.44 mg/g and the removal of metals were enhanced with increasing pH. The Freundlich model was adopted to depict the isotherms. The kinetic constants with pseudo-second-order model were 0.056 and 0.232 g/(mg·min), respectively, obtained from adsorption of $Cr^{3+}$ and $Cu^{2+}$. The thermodynamic analysis results demonstrated that the adsorption mechanism for $Cr^{3+}$ and $Cu^{2+}$ using FA-$Fe_3O_4$ was endothermic and spontaneous. Based on the excellent reusability of FA-$Fe_3O_4$, this study demonstrates a novel method for environmentally friendly removal of aquatic metals, with easier separation.

*Keywords:* Metal cations; Fulvic acid; Magnetic nanoparticle; Adsorption; Kinetics

## 1. Introduction

Water pollution with high concentrations of metals in surface water and groundwater has aroused much attention in recent years [1]. Heavy metals can accumulate in living organisms in an aquatic environment, causing many diseases and posing a great threat to the ecosystem and human health [2]. Based on strict environmental regulations and the potential toxicity, it is of great importance to develop alternative technologies for heavy metals removal [3]. Copper(II) and chromium(VI) are considered to be of most acute concern by World Health Organization [4]. Copper exists in water environments in a stable cupric state, while chromium emerges primarily in trivalent chromium ($Cr^{3+}$) and hexavalent chromium ($Cr^{6+}$). Although trivalent chromium is usually attributed to be a less toxic species compared with the hexavalent chromium, it could vulnerably be oxidized to hexavalent chromium [5]. Therefore, the removal of trivalent chromium is essential to control the concentration of hexavalent chromium. Further, trivalent chromium has been correlated with genotoxic side effects and apoptosis in previous studies [6,7]. Conventional treatments for heavy metals in industrial sewage consist of precipitation, ion-exchange, membrane filtration, electrochemical methods, reverse osmosis, solvent extraction and adsorption [8–12]. However, most of the methods seem limited due to the high operational cost

* Corresponding author.

and/or may also being inefficient for the lower concentration levels [13].

Adsorption technology has been considered as an alternative method for water decontamination concerning heavy metals in recent years due to the simple operation and relatively low cost. Recently, various types of adsorbents have been adopted for metallic decontamination, such as activated carbons, zeolites, lignocelluloses, clays and magnetic nanoparticles [14–19]. Iron magnetic nanoparticles, with the large specific surface area contributing to the adsorption capacity, are beneficial in separating from aqueous media. However, the bare iron magnetic nanoparticles tend to aggregate in response to the high surface energies as well as being vulnerable for auto-oxidation at ambient temperature [20]. A great number of magnetite-organic materials (defined as $Fe_3O_4$@organic) have recently been developed and adopted for the adsorption of metals in aquatic solutions, such as $Fe_3O_4$@chitosan, $Fe_3O_4$@humic acid, $Fe_3O_4$@polypyrrole and $Fe_3O_4$@vanillin [21–24], in proving enhancement of the adsorption capability for the target metal removal. It has been demonstrated that the surface functionalization using organic materials can efficiently avoid agglomeration and can maintain stability for magnetic nanoparticles [25]. Fulvic acid (FA), as a major humic substance component, is extensively distributed in soils, sediments and waters, with more oxygen-containing functional groups compared with humic acid [26,27]. Recent studies have indicated that FA was attributed to the sorption of heavy metals onto $\alpha$-$Fe_2O_3$, forming monodentate complexes [28,29]. However, to our best knowledge, limited research has been conducted using FA as a surface functionalization material to prepare magnetic nanoadsorbents for metallic decontamination in the water.

In the present study, a novel and facile magnetic adsorbent was prepared by coating $Fe_3O_4$ magnetic nanoparticles with fulvic acid (FA-$Fe_3O_4$) for heavy metals removal from aqueous solutions. Fourier transform infrared (FTIR), X-ray powder diffraction (XRD), scanning electron microscopy (SEM), thermogravimetric (TG) and Brunauer–Emmett–Teller (BET) were applied to characterize the physical and chemical features of FA-$Fe_3O_4$. The application of FA-$Fe_3O_4$ in the removal of $Cu^{2+}$ and $Cr^{3+}$ was evaluated in view of the adsorption kinetics and isotherms. The crucial parameters were investigated as well as the material reusability.

## 2. Materials and methods

### 2.1. Chemicals

Ferrous chloride tetrahydrate ($FeCl_2{\cdot}4H_2O$), ferric chloride hexahydrate ($FeCl_3{\cdot}6H_2O$), chromic nitrate nonahydrate ($Cr(NO_3)_3{\cdot}9H_2O$), cupric nitrate trihydrate ($Cu(NO_3)_2{\cdot}3H_2O$), ammonium hydroxide, hydrochloric acid, sodium hydroxide were AR grade, and were purchased from the open market in China. FA was purchased from Jianglai Biologics Co., Ltd. (Shanghai). All the solutions were prepared with ultrapure water (18.2 M/Ωcm).

### 2.2. Synthesis of bare $Fe_3O_4$ and FA coated $Fe_3O_4$

The bare $Fe_3O_4$ and FA coated $Fe_3O_4$ nanoparticles were synthesized according to a previous study [30]. Briefly, 12.2 g of $FeCl_3{\cdot}6H_2O$ and 6.0 g of $FeCl_2{\cdot}4H_2O$ were dissolved in 200 mL water. The mixed solution was heated to 90°C in a 500 mL round-bottom flask equipped with a reflux condenser. Then, 20 mL of 25% ammonium hydroxide and 100 mL of 3.0% FA solution were added to the mixture rapidly and sequentially. The reaction solution was aged at 90°C for an additional 30 min and then cooled to ambient temperature. The reaction solution was mechanically stirred throughout the whole reaction process. After being separated from the solution, the black precipitate was washed with water and dried for 12 h in a freeze dryer. Bare $Fe_3O_4$ was synthesized by the method mentioned above, in which 100 mL of water was alternatively added instead. The prepared $Fe_3O_4$ and FA-$Fe_3O_4$ nanoparticles were then ready for the adsorption experiments.

### 2.3. Experiments of adsorption

In a typical adsorption procedure, 0.1 g of FA-$Fe_3O_4$ was added to 50 mL of solution containing 25 mg/L $Cr^{3+}$ and $Cu^{2+}$, respectively. The solution pH was adjusted to fixed value by using 0.1 M NaOH and HCl. The experiments were carried out in an orbit shaker with continuous mixing at 250 rpm in a water bath environment. Then, the FA-$Fe_3O_4$ and the adsorbed metals were separated from the solution with a permanent hand-held magnet. The $Cr^{3+}$ and $Cu^{2+}$ in the solution were measured using an atomic absorption spectrophotometer (AAS-900T, PerkinElmer, Germany). The below equation was used to calculate the adsorption capability:

$$Q_t = V \cdot (C_0 - C_t)/m \tag{1}$$

where $Q_t$ is the adsorption capacity at time $t$ (mg/g); $C_0$ is the initial concentration of metals solution (mg/L); $C_t$ is the concentration of metals solution at time $t$ (mg/L); $m$ is the mass of the adsorbent added (g) and $V$ is the total volume of the metals solution (L).

### 2.4. Reusability experiment

Reusability experiments were conducted in a batch mode. FA-$Fe_3O_4$@Cr and FA-$Fe_3O_4$@Cu obtained in the adsorption were dispersed into 50 mL of 0.1 M HCl solutions in a thermostatic shaker for 2 h at 25°C. The regenerated adsorbent was collected by a hand-held magnet, washed to a neutral condition with deionized water and dried for 12 h in a freeze dryer before being reused. The adsorption–desorption process was repeated over three cycles.

### 2.5. Characterization

SEM measurements were run using a JSM-7500F (JEOL, Japan) at 20 kV, to determine the morphology of the FA-$Fe_3O_4$ nanoparticles. FTIR spectra of the bare $Fe_3O_4$ or the FA-$Fe_3O_4$ nanoparticles were conducted using a Nicolet iS10 FTIR spectrometer (Thermo Scientific, USA), with wavenumbers ranging from 400 to 4,000 $cm^{-1}$. The structure of the materials obtained was characterized by XRD spectrometry using an Empyrean diffractometer (PANalytical B.V., Holland). The thermal decomposition of the bare $Fe_3O_4$ and the FA-$Fe_3O_4$

was followed with a TG209F1 (Netzsch, Germany). Samples were placed in an alumina crucible and heated at 10°C/min from 30°C to 600°C in air. BET analysis was adopted using a JW-BK122F specific surface area analyzer (JWGB, China).

## 3. Results and discussion

### 3.1. Characterization of the synthesized samples

#### 3.1.1. FTIR analysis

FTIR spectra were first applied to verify the binding of FA on the $Fe_3O_4$ nanoparticles surface. It is seen in Fig. 1 that the peaks at 580 and 3,371 $cm^{-1}$ both appeared in the spectrum of the bare $Fe_3O_4$, FA-$Fe_3O_4$, FA-$Fe_3O_4$@Cr and FA-$Fe_3O_4$@Cu. The peak at 580 $cm^{-1}$ displays a stretching vibration of the Fe–O bonds, and the peak at 3,371 $cm^{-1}$ is attributed to –OH stretching vibration, which is inherent in the bare $Fe_3O_4$. In the spectrum of FA, peaks at 3,540 and 1,681 $cm^{-1}$ correspond to the vibration of hydroxyl and carboxyl, respectively. Since –OH stretching vibration for the bare $Fe_3O_4$ is weaker than that of FA-$Fe_3O_4$, it indicated that the hydrogen-bonding contributed to the connection between FA and $Fe_3O_4$ [21,29]. The observed peak at 1,612 $cm^{-1}$ is assigned to the C=O stretches of FA-$Fe_3O_4$, demonstrating the binding of the carboxylate from the FA on the $Fe_3O_4$ surface. Compared with the bare $Fe_3O_4$, the transmittance of C=O had a significant increase and the IR band of C=O had a red shift for the typical peak that emerged at 1,700 $cm^{-1}$ [3,30]. The vibration bands at 1,405 and 1,313 $cm^{-1}$ were newly observed in FA-$Fe_3O_4$, which are respectively associated with the in-plane N–H in amide groups and –OH in hydroxyl groups [31]. In addition, multiple peaks observed between 900 and 1,200 $cm^{-1}$ were likely attributable to the other organic chemical bonds in FA (such as –COOR, –$CH_2$). The appearance of the typical peaks in the spectrum of FA-$Fe_3O_4$ showed the coating success of FA compared with the bare $Fe_3O_4$. Of note, peaks at 1,612, 1,405 and 1,313 $cm^{-1}$ in FA-$Fe_3O_4$@Cr and FA-$Fe_3O_4$@Cu are weakened compared with FA-$Fe_3O_4$, indicating the adsorption of $Cr^{3+}$ and $Cu^{2+}$ is a cooperation of carboxyl, amino and hydroxyl groups. The invariable peaks between 900 and 1,200 $cm^{-1}$ demonstrated the high binding affinity of FA onto $Fe_3O_4$ and simple desorption in the solutions is difficult [32].

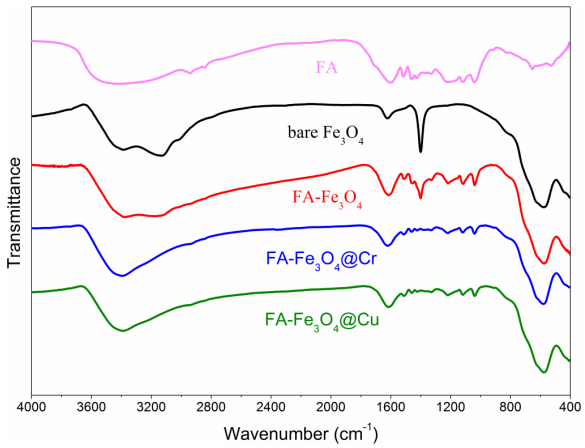


Fig. 1. FTIR spectra of the synthesized materials under various conditions.

#### 3.1.2. XRD analysis

XRD was employed to characterize the crystalline structure of FA-$Fe_3O_4$, FA-$Fe_3O_4$@Cr and FA-$Fe_3O_4$@Cu, and the results are shown in Fig. 2. The diffraction peaks at 30.1, 35.6, 43.3, 57.28 and 62.80 correspond to the (220), (311), (400), (511) and (440) planes. The position of the peaks was in accordance with literature showing typical diffraction peaks of $Fe_3O_4$ (JCPDS No. 85-1436) [33,34]. This result suggests that the phase and structure of the $Fe_3O_4$ core are not altered by the FA coating, revealing the well-known spinel structure of magnetite materials. Previous reports indicated that the Fe(II) present in magnetite was susceptible to auto-oxidation forming Fe(III) materials with reduced magnetic properties [35,36], while the unchanged peaks in FA-$Fe_3O_4$@Cr and FA-$Fe_3O_4$@Cu demonstrated the advantage of antioxidant FA-$Fe_3O_4$ in heavy metals adsorption.

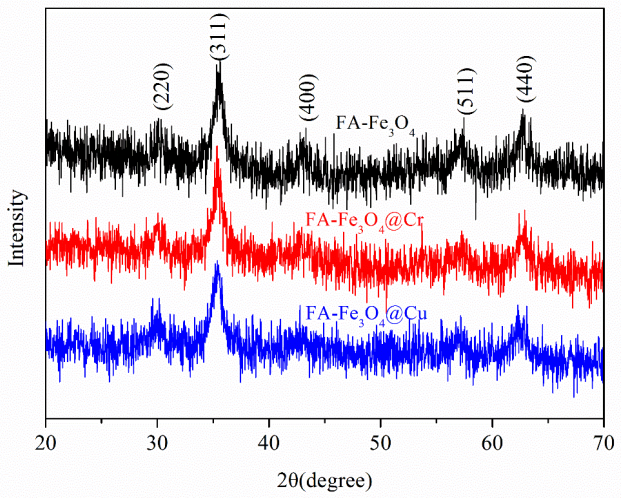


Fig. 2. XRD patterns of FA-$Fe_3O_4$, FA-$Fe_3O_4$@Cr and FA-$Fe_3O_4$@Cu.

#### 3.1.3. SEM analysis

SEM was used to observe the morphologies of the prepared FA-$Fe_3O_4$ magnetic nanoparticles with the images presented in Fig. 3. It can be clearly seen that the preparation of FA-$Fe_3O_4$ did not change the basically spherical morphology of $Fe_3O_4$ and the average size ranged from 10 to 15 nm, which is similar to the results of previous research [3].

#### 3.1.4. TG analysis

TG analysis was applied to estimate the proportion of FA in the obtained FA-$Fe_3O_4$ composite. The weight loss curves of the bare $Fe_3O_4$ and FA-$Fe_3O_4$ at temperatures ranging from 30°C to 600°C are shown in Fig. 4. The weights of the two samples decrease slowly and sequentially with the temperature elevations. It can be calculated from the ultimate loss curves that the FA constituted approximately 18.3% of the FA-$Fe_3O_4$ composite. In addition, the weight loss observed below 50°C in the two samples suggests that only a 3.36% weight loss was observed, which is acceptable in conventional water treatment.

### 3.1.5. BET analysis

The nitrogen adsorption–desorption measurements were conducted for the FA-$Fe_3O_4$ with the isotherm data illustrated in Fig. 5. According to the classification of the International Union of Pure and Applied Chemistry, the isotherms are type IV provided by many mesoporous industrial adsorbents, characteristic of mesoporous structures [37]. The specific surface area of the bare $Fe_3O_4$ is 51.97 $m^2/g$ with a total pore volume of 0.24 $cm^3/g$. For FA-$Fe_3O_4$, a similar specific surface area of 55.16 $m^2/g$ and a higher total pore volume of 0.46 $cm^3/g$ were obtained. The increased total pore volume can contribute to the adsorption capability, while the similar surface area might be attributed to the fact that FA has a very narrow microporosity with limited $N_2$ adsorption (less than 1 $m^2/g$) at 77 K [38].

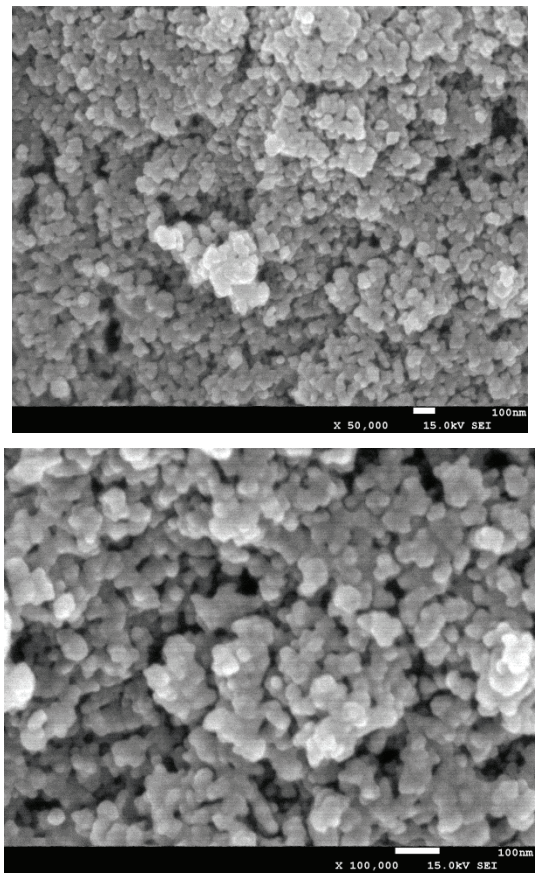


Fig. 3. SEM images of FA-$Fe_3O_4$.

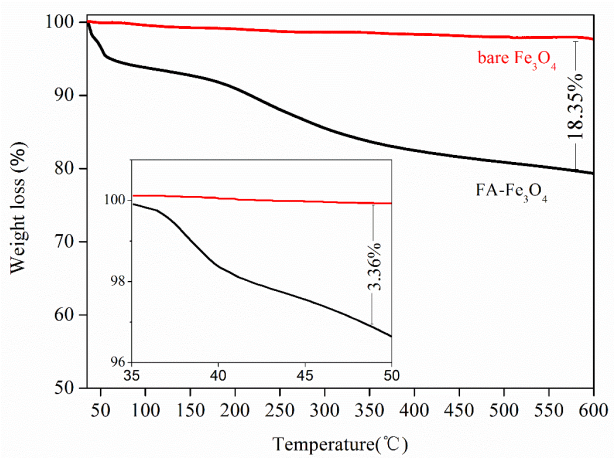


Fig. 4. Thermal decomposition curves for $Fe_3O_4$ and FA-$Fe_3O_4$.

## 3.2. Adsorption performance

### 3.2.1. Effect of initial pH

According to previous studies, $Cr^{3+}$ can form $Cr(OH)_3$ and precipitate when the pH rises over 6.0 [39,40]. Based on this, the solution pH was adjusted in the range of 3.0–5.0, in which cupric and chromium were both in ionic forms. The adsorption capability for $Cr^{3+}$ and $Cu^{2+}$ at different pH are given in Fig. 6, showing the increasing adsorption capacity for $Cr^{3+}$ (4.01–8.31 mg/g) and $Cu^{2+}$ (1.86–2.94 mg/g), and can be explained with the adsorption sites on the adsorbent and the surface potential of the adsorbent. However, the adsorption equilibrium time is nearly invariant with the pH variations. On the one hand, FA has an acid group with a p$K_a$ between 2.0 and 5.0, corresponding to carboxylic-like functionality [41].

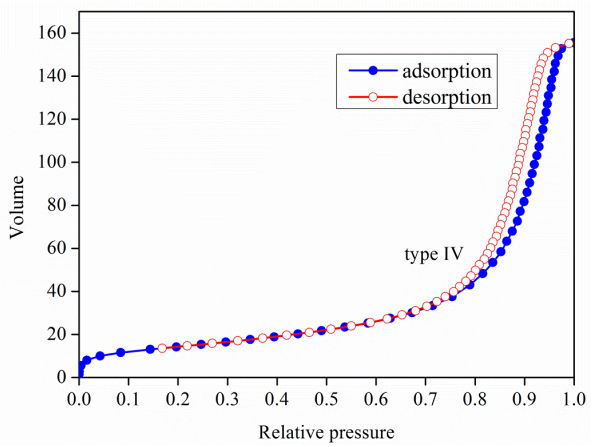


Fig. 5. $N_2$ adsorption–desorption isotherms of FA-$Fe_3O_4$.

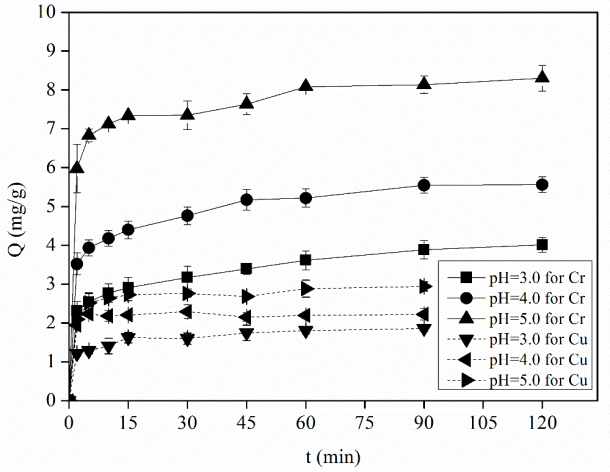


Fig. 6. Effect of pH on removal efficiency of $Cr^{3+}$ and $Cu^{2+}$ by FA-$Fe_3O_4$ ([metal] = 25 mg/L, adsorbent dose = 2 g/L).

At lower pH values, carboxylic-like groups in the FA-$Fe_3O_4$ are predominantly protonated, and with increasing pH, these functional groups, as important ligands, are dissociated and deprotonated to provide more adsorption sites for the complexation of heavy metals. On the other hand, it was reported that the $pH_{pzc}$ of humic substance-coating-magnetite was below 3.0, indicating the prepared FA-$Fe_3O_4$ had a negative surface charge for the selected range of pH [3,42]. At the higher pH values, the electrostatic interaction was enhanced between the FA-$Fe_3O_4$ with negatively charged surface ligands (amino and hydroxyl groups) and metal cations. Based on Fig. 6, it can be concluded that the contribution of FA in removing $Cr^{3+}$ and $Cu^{2+}$ are pH dependent and more efficient at higher pH. Consequently, the following experiments were carried out at the optimum pH.

### 3.2.2. Contact time and adsorption kinetics

Kinetic experiments were conducted in a batch mode, 0.1 g FA-$Fe_3O_4$ was added into 50 mL solution containing 25 mg/L metallic ions. FA-$Fe_3O_4$ with the adsorbed metals were separated from the solution by a hand-held magnet within a few seconds due to the excellent magnetic performance, and the obtained samples at fixed time intervals were analyzed over 12 h. As shown in Fig. 7, the FA-$Fe_3O_4$ has a higher adsorption capacity than the bare $Fe_3O_4$, confirming the advantage of modifying $Fe_3O_4$ with FA. Of note, the adsorption occurs rapidly during the early stage (in the first 15 min) due to the high number of available adsorption sites on the surface functional groups of FA-$Fe_3O_4$, and the high metal concentration gradient. Subsequently, the adsorption rate becomes slower and remains unchangeable after 90–120 min, indicating that most of the adsorption sites have been saturated [24,43]. The pseudo-first-order kinetics equation and pseudo-second-order kinetics equation were adopted to fit the adsorption model for metal removal using the following equations [44]:

$$\lg(Q_e - Q_t) = \lg Q_e - k_1 t / 2.303 \tag{2}$$

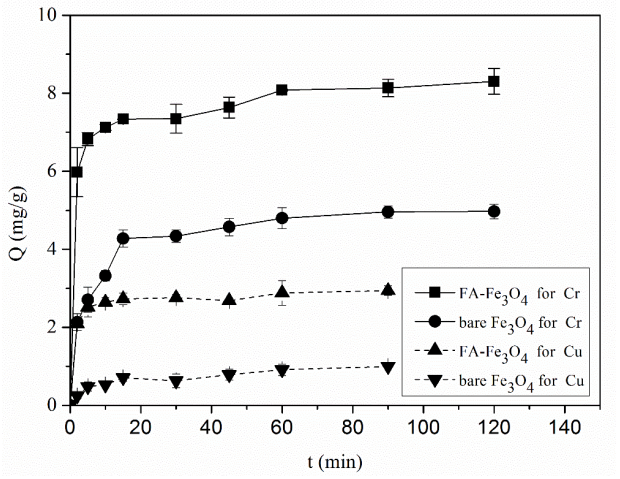


Fig. 7. Effect of adsorption time on removal efficiency of $Cr^{3+}$ and $Cu^{2+}$ ([metal] = 25 mg/L, adsorbent dose = 2 g/L, pH = 5.0).

$$t / Q_t = (k_2 Q_e^{\,2})^{-1} + t / Q_e \tag{3}$$

Here $Q_e$ represents adsorption capacity at equilibrium (mg/g); $k_1$ and $k_2$ are the rate parameters of the pseudo-first-order and pseudo-second-order, respectively.

Both $Cr^{3+}$ and $Cu^{2+}$ received a poor fitting with pseudo-first-order kinetics (data not shown), with a excellent fitting for pseudo-second-order kinetics (shown in Fig. 8, $R^2$> 0.99). It was demonstrated that the adsorption processes of $Cr^{3+}$ and $Cu^{2+}$ onto FA-$Fe_3O_4$ tended to be a chemical interaction owing to the complexation between the metal ions and functional groups of FA [45,46]. The whole adsorption process consists of two distinct parts. First, a rapid grab occurred on the external surface of FA-$Fe_3O_4$ because of the large number of available adsorption sites on the surface functional groups of FA-$Fe_3O_4$ and the high concentration gradient. The subsequent slow adsorption is attributed to the longer diffusion range of metal irons through the inner-sphere pores of the adsorbents.

### 3.2.3. Adsorption isotherms

Several experiments were conducted to verify the adsorption isotherms for the removal of metals using the obtained composite. The Langmuir model presumes monolayer adsorption occurs on the adsorbent surface, while the Freundlich model presumes multilayer adsorption, calculated by the following equations, respectively [47,48].

$$1 / Q_e = (Q_m K_L)^{-1} / C_e + 1 / Q_m \tag{4}$$

$$\ln Q_e = n^{-1} \ln C_e + \ln K_F \tag{5}$$

Here $C_e$ (mg/L) and $Q_e$ (mg/g) represent the residual concentration and adsorption capacity at equilibrium; $Q_m$ is the maximum adsorption capacity in theory and $K_L$ is the Langmuir constant responding to the adsorption energy. $K_F$ and $n^{-1}$, the Freundlich constants correspond to the adsorption capacity and intensity.

Based on Eqs. (4) and (5), the Langmuir and Freundlich models were, respectively, fitted and the parameters for the isotherm are shown in Table 1. This result suggests that the adsorption of $Cr^{3+}$ by FA-$Fe_3O_4$ is preferably fitted using the Freundlich model, while the adsorption of $Cu^{2+}$ can be described by both the Langmuir and Freundlich model. The discrepancy in bonding energy between Cr-coordination and Cu-coordination might contribute to the obtained results. In addition, the maximum adsorption capacity ($q_{max}$) has been theoretically calculated from the Langmuir model.

Table 1
Estimated Langmuir and Freundlich isothermal parameters for the adsorption of $Cr^{3+}$ and $Cu^{2+}$ onto FA-$Fe_3O_4$ at pH 5.0

| Adsorbates | Langmuir isotherms | | | Freundlich isotherms | | |
|---|---|---|---|---|---|---|
| | $K_L$ | $Q_m$ | $R^2$ | $K_F$ | $n$ | $R^2$ |
| $Cr^{3+}$ | 0.296 | 11.587 | 0.824 | 2.949 | 1.988 | 0.884 |
| $Cu^{2+}$ | 0.022 | 3.442 | 0.933 | 0.014 | 0.564 | 0.931 |

The maximum adsorption capacity and equilibrium time for various adsorbents reported are summarized and shown in Table 2, confirming that FA-$Fe_3O_4$ is more efficient than other adsorbents.

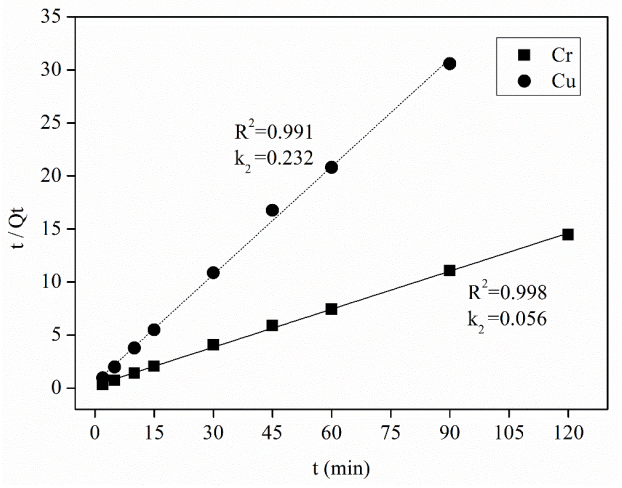


Fig. 8. Pseudo-second-order for $Cr^{3+}$ and $Cu^{2+}$ adsorption onto FA-$Fe_3O_4$ ([metal] = 25 mg/L, adsorbent dose = 2 g/L, pH = 5.0).

Table 2
Comparison of Langmuir maximum adsorption capacity by various adsorbents at 298 K

| Adsorbents | $Q_m$ (mg/g) | Equilibrium time (h) | Reference |
|---|---|---|---|
| R-CNTs | 0.37 | 1.5 | [49] |
| M-CNTs | 0.50 | 2.0 | [49] |
| Oxidized multiwalled carbon nanotubes | 2.60 | 28.0 | [50] |
| Biofunctional magnetic beads | 5.79 | 12.0 | [51] |
| Polypyrrole/wood sawdust | 3.4 | 0.16 | [52] |
| Fulvic acid coated $Fe_3O_4$ for Cr | 11.59 | 2.0 | This study |
| Fulvic acid coated $Fe_3O_4$ for Cu | 3.44 | 1.5 | This study |

*3.2.4. Adsorption thermodynamics*

To study the energy change during the reaction process, thermodynamic analysis was used for the removal of metal ions using FA-$Fe_3O_4$. FA-$Fe_3O_4$ (0.1 g) was added into a 50 mL solution containing 25 mg/L metallic ions, and the adsorption was conducted in the range of 298–318 K. The thermodynamic parameters $\Delta H°$, $\Delta S°$ and $\Delta G°$ were evaluated by following equations [53]:

$$\Delta G^0 = \Delta H^0 - T\Delta S^0 \quad (6)$$

$$\ln K = -\frac{\Delta H^0}{RT} + \frac{\Delta S^0}{R} \quad (7)$$

where $K$ is the thermodynamic equilibrium constant and $R$ is the gas constant with a value of 8.314 J/mol·K.

Fig. 9 shows the plots of ln$K$ vs. 1/$T$ based on Eqs. (5) and (6). The thermodynamic values were obtained and presented in Table 3. For the selected range of temperature, all the $\Delta G°$ values for both $Cr^{3+}$ and $Cu^{2+}$ are negative, indicating a spontaneous and feasible process for the adsorption in water treatment [54]. In addition, the positive $\Delta H°$ and $\Delta S°$ values for $Cr^{3+}$ and $Cu^{2+}$ confirm the endothermic nature and the increasing randomness of the adsorption process at the solid–solution interface [55].

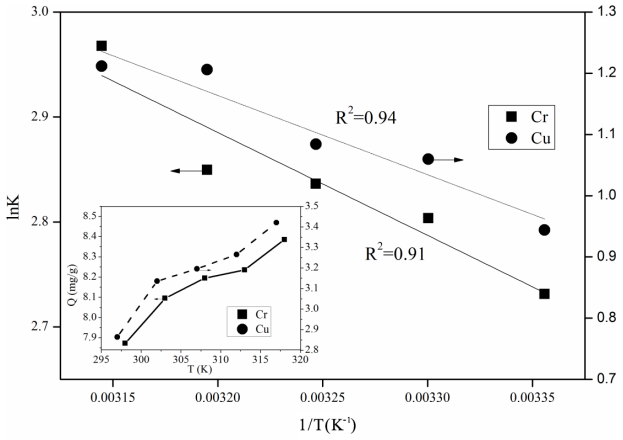


Fig. 9. Estimation of thermodynamic parameters with the relevant experimental curves at various temperatures ([metal] = 25 mg/L, adsorbent dose = 2 g/L, pH = 5.0).

Table 3
Estimated thermodynamic parameters for the adsorption of $Cr^{3+}$ and $Cu^{2+}$ onto FA-$Fe_3O_4$

| $T$ (K) | Adsorption of $Cr^{3+}$ | | | Adsorption of $Cu^{2+}$ | | |
|---|---|---|---|---|---|---|
| | $\Delta G°$ (kJ/mol) | $\Delta H°$ (kJ/mol) | $\Delta S°$ (J/mol·K) | $\Delta G°$ (kJ/mol) | $\Delta H°$ (kJ/mol) | $\Delta S°$ (J/mol·K) |
| 298 | –6.771 | 8.153 | 50.082 | –2.384 | 10.767 | 44.131 |
| 303 | –7.022 | | | –2.605 | | |
| 308 | –7.272 | | | –2.825 | | |
| 313 | –7.523 | | | –3.046 | | |
| 318 | –7.773 | | | –3.267 | | |

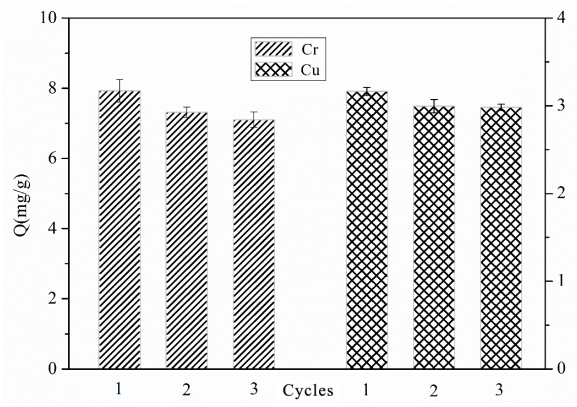


Fig. 10. Reusability of FA-$Fe_3O_4$ for the adsorption of $Cr^{3+}$ and $Cu^{2+}$ ([metal] = 25 mg/L, adsorbent dose = 2 g/L, pH = 5.0).

*3.2.5. Desorption and regeneration*

The reusability of an adsorbent is an essential factor for actual applications. In our study, the desorption experiments were carried out by dispersing exhausted FA-$Fe_3O_4$ into 50 mL desorbent (0.1 M HCl), and keeping agitating for 2 h at 25°C. The regenerated adsorbent was then collected by a hand-held magnet, and washed to neutral condition with deionized water. The adsorption–desorption process was repeated over three cycles [23,56]. As illustrated in Fig. 10, FA-$Fe_3O_4$ maintained a stable adsorption capacity for $Cr^{3+}$ and $Cu^{2+}$, with slightly reduction (less than 10%) after the three cycles, which proved the economical value as an adsorbent for metallic decontamination in water.

## 4. Conclusions

In this study, FA-$Fe_3O_4$ nanoparticles were synthesized, characterized and applied to remove $Cr^{3+}$ and $Cu^{2+}$ in an aqueous solution. Several crucial factors were elucidated in the metallic decontamination. The prepared FA-$Fe_3O_4$ was all the nanoscale with an average size of 15 nm and a specific surface area of 55.16 $m^2/g$. By coating with FA, the FA-$Fe_3O_4$ was dispersive and stable in aqueous solution, exhibiting remarkable enhancement for heavy metal removal. This study revealed that the removal efficiency was relatively high at the initial state of the adsorption and strengthened with increasing pH. The adsorption data were well fitted by pseudo-second-order kinetics and the Freundlich isotherms. The values of $\Delta H°$ and $\Delta S°$ were respectively calculated as 8.153 kJ/mol and 50.082 J/mol·K for $Cr^{3+}$, and 10.767 kJ/mol and 44.131 J/mol·K for $Cu^{2+}$. The excellent reusability results for the synthesized material indicates promising applicability for removing metals from aqueous solutions.

## Acknowledgements

This work was financially supported by the National Natural Science Foundation of China (51508354), China Postdoctoral Science Foundation (2016M590888) and the Project of Science & Technology Bureau of Chengdu (2015-HM01-00502-SF). The authors are thankful to all the anonymous reviewers for their insightful comments and suggestions.

## References

[1] J.O. Nriagu, J.M. Pacyna, Quantitative assessment of worldwide contamination of air, water and soils by trace-metals, Nature, 333 (1988) 134–139.
[2] G.R. MacFarlane, M.D. Burchett, Toxicity, growth and accumulation relationships of copper, lead and zinc in the grey mangrove *Avicennia marina* (Forsk.) Vierh, Mar. Environ. Res., 54 (2002) 65–84.
[3] J.F. Liu, Z.S. Zhao, G.B. Jiang, Coating $Fe_3O_4$ magnetic nanoparticles with humic acid for high efficient removal of heavy metals in water, Environ. Sci. Technol., 42 (2008) 6949–6954.
[4] G.P. Broom, R.C. Squires, M.P.J. Simpson, I. Martin, The treatment of heavy-metal effluents by cross-flow microfiltration, J. Membr. Sci., 87 (1994) 219–230.
[5] A. Bedemo, B.S. Chandravanshi, F. Zewge, Removal of trivalent chromium from aqueous solution using aluminum oxide hydroxide, Springerplus, 5 (2016) 1288.
[6] A. Levina, P.A. Lay, Chemical properties and toxicity of chromium(III) nutritional supplements, Chem. Res. Toxicol., 21 (2008) 563–571.
[7] R. Rajaram, B.U. Nair, T. Ramasami, Chromium(III) induced abnormalities in human lymphocyte cell-proliferation: evidence for apoptosis, Biochem. Biophys. Res. Commun., 210 (1995) 434–440.
[8] K.G. Karthikeyan, H.A. Elliott, F.S. Cannon, Adsorption and coprecipitation of copper with the hydrous oxides of iron and aluminum, Environ. Sci. Technol., 31 (1997) 2721–2725.
[9] J.B. Brower, R.L. Ryan, M. Pazirandeh, Comparison of ion-exchange resins and biosorbents for the removal of heavy metals from plating factory wastewater, Environ. Sci. Technol., 31 (1997) 2910–2914.
[10] C. Blocher, J. Dorda, V. Mavrov, H. Chmiel, N.K. Lazaridis, K.A. Matis, Hybrid flotation—membrane filtration process for the removal of heavy metal ions from wastewater, Water Res., 37 (2003) 4018–4026.
[11] C.A. Basha, N.S. Bhadrinarayana, N. Anantharaman, K.M.M.S. Begum, Heavy metal removal from copper smelting effluent using electrochemical cylindrical flow reactor, J. Hazard. Mater., 152 (2008) 71–78.
[12] H. Abu Qdais, H. Moussa, Removal of heavy metals from wastewater by membrane processes: a comparative study, Desalination, 164 (2004) 105–110.
[13] M. Monier, D.M. Ayad, A.A. Sarhan, Adsorption of Cu(II), Hg(II), and Ni(II) ions by modified natural wool chelating fibers, J. Hazard. Mater., 176 (2010) 348–355.
[14] J. Goel, K. Kadirvelu, C. Rajagopal, V.K. Garg, Removal of lead(II) by adsorption using treated granular activated carbon: batch and column studies, J. Hazard. Mater., 125 (2005) 211–220.
[15] P. Shekinah, K. Kadirvelu, P. Kanmani, P. Senthilkumar, V. Subburam, Adsorption of lead(II) from aqueous solution by activated carbon prepared from *Eichhornia*, J. Chem. Technol. Biotechnol., 77 (2002) 458–464.
[16] X.X. Wang, D.D. Shao, G.S. Hou, X.K. Wang, A. Alsaedi, B. Ahmad, Uptake of Pb(II) and U(VI) ions from aqueous solutions by the ZSM-5 zeolite, J. Mol. Liq., 207 (2015) 338–342.
[17] C. Saka, O. Sahin, M.M. Kucuk, Applications on agricultural and forest waste adsorbents for the removal of lead(II) from contaminated waters, Int. J. Environ. Sci. Technol., 9 (2012) 379–394.
[18] Z. Reddad, C. Gerente, Y. Andres, P. Le Cloirec, Adsorption of several metal ions onto a low-cost biosorbent: kinetic and equilibrium studies, Environ. Sci. Technol., 36 (2002) 2067–2073.
[19] D.A. Glatstein, F.M. Francisca, Influence of pH and ionic strength on Cd, Cu and Pb removal from water by adsorption in Na-bentonite, Appl. Clay Sci., 118 (2015) 61–67.
[20] D. Maity, D.C. Agrawal, Synthesis of iron oxide nanoparticles under oxidizing environment and their stabilization in aqueous and non-aqueous media, J. Magn. Magn. Mater., 308 (2007) 46–55.
[21] Y.C. Chang, D.H. Chen, Preparation and adsorption properties of monodisperse chitosan-bound $Fe_3O_4$ magnetic nanoparticles

for removal of Cu(II) ions, J. Colloid Interface Sci., 283 (2005) 446–451.
[22] S.T. Yang, P.F. Zong, X.M. Ren, Q. Wang, X.K. Wang, Rapid and highly efficient preconcentration of Eu(III) by core-shell structured $Fe_3O_4$@humic acid magnetic nanoparticles, ACS Appl. Mater. Interfaces, 4 (2012) 6890–6899.
[23] M. Bhaumik, A. Maity, V.V. Srinivasu, M.S. Onyango, Enhanced removal of Cr(VI) from aqueous solution using polypyrrole/$Fe_3O_4$ magnetic nanocomposite, J. Hazard. Mater., 190 (2011) 381–390.
[24] D.C. Culita, C.M. Simonescu, R.E. Patescu, M. Dragne, N. Stanica, O. Oprea, o-Vanillin functionalized mesoporous silica – coated magnetite nanoparticles for efficient removal of Pb(II) from water, J. Solid State Chem., 238 (2016) 311–320.
[25] W. Wu, Q.G. He, C.Z. Jiang, Magnetic iron oxide nanoparticles: synthesis and surface functionalization strategies, Nanoscale Res. Lett., 3 (2008) 397–415.
[26] J. Morales, J.A. Manso, A. Cid, J.C. Mejuto, Degradation of carbofuran and carbofuran-derivatives in presence of humic substances under basic conditions, Chemosphere, 89 (2012) 1267–1271.
[27] E.B.O. Gungor, M. Bekbolet, Zinc release by humic and fulvic acid as influenced by pH, complexation and DOC sorption, Geoderma, 159 (2010) 131–138.
[28] W.W. Tang, G.M. Zeng, J.L. Gong, J. Liang, P. Xu, C. Zhang, B.B. Huang, Impact of humic/fulvic acid on the removal of heavy metals from aqueous solutions using nanomaterials: a review, Sci. Total Environ., 468 (2014) 1014–1027.
[29] Q. Du, Z.X. Sun, W. Forsling, H.X. Tang, Complexations in illite-fulvic acid-$Cu^{2+}$ systems, Water Res., 33 (1999) 693–706.
[30] W.J. Jiang, Q. Cai, W. Xu, M.W. Yang, Y. Cai, D.D. Dionysiou, K.E. O'Shea, Cr(VI) adsorption and reduction by humic acid coated on magnetite, Environ. Sci. Technol., 48 (2014) 8078–8085.
[31] P. Luo, J.S. Zhang, B. Zhang, J.H. Wang, Y.F. Zhao, J.D. Liu, Preparation and characterization of silane coupling agent modified halloysite for Cr(VI) removal, Ind. Eng. Chem. Res., 50 (2011) 10246–10252.
[32] B.H. Gu, J. Schmitt, Z.H. Chen, L.Y. Liang, J.F. Mccarthy, Adsorption and desorption of natural organic-matter on iron-oxide – mechanisms and models, Environ. Sci. Technol., 28 (1994) 38–46.
[33] M.R. Lasheen, I.Y. El-Sherif, D.Y. Sabry, S.T. El-Wakeel, M.F. El-Shahat, Removal and recovery of Cr(VI) by magnetite nanoparticles, Desal. Wat. Treat., 52 (2014) 6464–6473.
[34] S.H. Sun, H. Zeng, Size-controlled synthesis of magnetite nanoparticles, J. Am. Chem. Soc., 124 (2002) 8204–8205.
[35] Y.T. He, S.J. Traina, Cr(VI) reduction and immobilization by magnetite under alkaline pH conditions: the role of passivation, Environ. Sci. Technol., 39 (2005) 4499–4504.
[36] S.R. Chowdhury, E.K. Yanful, Arsenic and chromium removal by mixed magnetite-maghemite nanoparticles and the effect of phosphate on removal, J. Environ. Manage., 91 (2010) 2238–2247.
[37] K.S.W. Sing, D.H. Everett, R.A.W. Haul, L. Moscou, R.A. Pierotti, J. Rouquerol, T. Siemieniewska, Reporting physisorption data for gas solid systems with special reference to the determination of surface-area and porosity (Recommendations 1984), Pure Appl. Chem., 57 (1985) 603–619.
[38] R.A. Alvarez-Puebla, P.J.G. Goulet, J.J. Garrido, Characterization of the porous structure of different humic fractions, Colloids Surf., A, 256 (2005) 129–135.
[39] D. Rai, B.M. Sass, D.A. Moore, Chromium(III) hydrolysis constants and solubility of chromium(III) hydroxide, Inorg. Chem., 26 (1987) 345–349.
[40] D. Rai, D.A. Moore, N.J. Hess, L. Rao, S.B. Clark, Chromium(III) hydroxide solubility in the aqueous $Na^+$-$OH^-$-$H_2PO_4^-$-$HPO_4^{2-}$-$PO_4^{3-}$-$H_2O$ system: a thermodynamic model, J. Solution Chem., 33 (2004) 1213–1242.
[41] M.Q. Yan, Q.W. Fu, D.C. Li, G.F. Gao, D.S. Wang, Study of the pH influence on the optical properties of dissolved organic matter using fluorescence excitation-emission matrix and parallel factor analysis, J. Lumin., 142 (2013) 103–109.
[42] J. Yu, F. Liu, M.Z. Yousaf, Y.L. Hou, Magnetic nanoparticles: chemical synthesis, functionalization and biomedical applications, Prog. Biochem. Biophys., 40 (2013) 903–917.
[43] L.J. Kennedy, J.J. Vijaya, G. Sekaran, K. Kayalvizhi, Equilibrium, kinetic and thermodynamic studies on the adsorption of m-cresol onto micro- and mesoporous carbon, J. Hazard. Mater., 149 (2007) 134–143.
[44] J. Febrianto, A.N. Kosasih, J. Sunarso, Y.H. Ju, N. Indraswati, S. Ismadji, Equilibrium and kinetic studies in adsorption of heavy metals using biosorbent: a summary of recent studies, J. Hazard. Mater., 162 (2009) 616–645.
[45] X.S. Wang, L. Zhu, H.J. Lu, Surface chemical properties and adsorption of Cu (II) on nanoscale magnetite in aqueous solutions, Desalination, 276 (2011) 154–160.
[46] H.K. Boparai, M. Joseph, D.M. O'Carroll, Kinetics and thermodynamics of cadmium ion removal by adsorption onto nano zerovalent iron particles, J. Hazard. Mater., 186 (2011) 458–465.
[47] Y. Liu, Some consideration on the Langmuir isotherm equation, Colloids Surf., A, 274 (2006) 34–36.
[48] C.H. Yang, Statistical mechanical study on the Freundlich isotherm equation, J. Colloid Interface Sci., 208 (1998) 379–387.
[49] M.A. Atieh, O.Y. Bakather, B.S. Tawabini, A.A. Bukhari, M. Khaled, M. Alharthi, M. Fettouhi, F.A. Abuilaiwi, Removal of chromium (III) from water by using modified and nonmodified carbon nanotubes, J. Nanomater., 2010 (2010) 1–9.
[50] J. Hu, C.L. Chen, X.X. Zhu, X.K. Wang, Removal of chromium from aqueous solution by using oxidized multiwalled carbon nanotubes, J. Hazard. Mater., 162 (2009) 1542–1550.
[51] H.D. Li, Z. Li, T. Liu, X. Xiao, Z.H. Peng, L. Deng, A novel technology for biosorption and recovery hexavalent chromium in wastewater by bio-functional magnetic beads, Bioresour. Technol., 99 (2008) 6271–6279.
[52] R. Ansari, N.K. Fahim, Application of polypyrrole coated on wood sawdust for removal of Cr(VI) ion from aqueous solutions, React. Funct. Polym., 67 (2007) 367–374.
[53] Y. Liu, Is the free energy change of adsorption correctly calculated?, J. Chem. Eng. Data, 54 (2009) 1981–1985.
[54] A. Ayati, B. Tanhaei, M. Sillanpaa, Lead(II)-ion removal by ethylenediaminetetraacetic acid ligand functionalized magnetic chitosan-aluminum oxide-iron oxide nanoadsorbents and microadsorbents: equilibrium, kinetics, and thermodynamics, J. Appl. Polym. Sci., 134 (2017) 44360.
[55] T. Singh, R. Singhal, Regenerable hydrogels based on poly(acrylic acid-sodium acrylate-acrylamide) modified by sodium humate for high removal of $Pb^{2+}$ and $Fe^{2+}$ ions: metal adsorption kinetics and thermodynamic studies, Desal. Wat. Treat., 52 (2014) 5611–5628.
[56] X.Y. Guan, J.M. Chang, Y. Chen, H.J. Fan, A magnetically-separable $Fe_3O_4$ nanoparticle surface grafted with polyacrylic acid for chromium(III) removal from tannery effluents, RSC Adv., 5 (2015) 50126–50136.